

# Picosecond spectroscopy of nonlinear optical activity and nonlinear absorption in gallium arsenide

S. A. Akhmanov, N. I. Zheludev, and R. S. Zadoyan

*M. V. Lomonosov State University, Moscow*

(Submitted 13 February 1986)

Zh. Eksp. Teor. Fiz. **91**, 984–1000 (September 1986)

Polarization spectroscopy techniques are used to analyze the dispersion of the nonlinear anisotropy and nonlinear gyrotropy near one- and two-photon interband resonances in a gallium arsenide crystal. A picosecond polarimeter-densitometer is developed which is capable of measuring the frequency dependence of the nonlinear rotation of the plane of polarization accurate to  $10^{-4}$  rad in the  $0.7\text{--}2\ \mu\text{m}$  range. A technique for distinguishing the nonlinear anisotropy and nonlocality effects is developed which is based on analyzing the orientation and dispersion dependences of the nonlinear rotation. New data on the latent anisotropy of the GaAs crystal lattice and on the band structure are obtained by measuring the dispersion of the anisotropy in the cubic susceptibility. An exciton resonance was recorded in the nonlinear gyrotropy, and a "giant" nonlinear polarization self-action at one-photon exciton resonance was detected. Data are presented on the contribution of higher nonlinearities (saturation of the cubic susceptibilities in strong fields).

## 1. ANISOTROPY AND NONLOCAL NATURE OF THE NONLINEAR RESPONSE; POLARIZATION SELF-ACTION

In this paper we discuss some spectroscopic applications of the phenomenon of the polarization self-action of light, or nonlinear optical activity (NOA) as it is called in the literature. In the simplest case, NOA causes the rotation angle of the polarization plane of linearly polarized light to depend on the intensity. The term "nonlinear optical activity" was first used to refer to the change in the natural gyrotropy of a medium induced by a strong light field (we will call this NOA-1).<sup>1</sup> The intensity dependence of the NOA can be illustrated by considering the classical model of an ensemble of molecules that consist of coupled orthogonal oscillators separated by a distance  $D$  that determines the characteristic scale of the spatial dispersion in the medium. The specific rotational power  $d\varphi/dz$  of an ensemble of randomly oriented molecules of this type is known<sup>2</sup> to be proportional to the size of the molecules (the distance between the oscillators), to the oscillator coupling constant  $\xi$ , and to a resonance factor that depends on the difference between the excitation frequency  $\omega$  and the frequency  $\tilde{\omega}$  of the electron absorption band:

$$d\varphi/dz \propto D\xi\omega^2/(\tilde{\omega}^2 - \omega^2)^2. \quad (1)$$

Here  $\varphi$  is the rotation angle of the polarization plane and  $z$  is the coordinate along the direction of propagation of the light. A strong light field can induce anharmonic vibrations in the molecule and thereby alter the equilibrium distance between individual chromophore centers, shift the absorption resonance, or change the elastic constant for the coupling between the oscillators. In all of these cases, the rotational power of the medium becomes dependent on the intensity of the light, which causes the nonlinear response to become nonlocal.

In addition to the nonlinear optical activity due to nonlocal nature of the nonlinear response, there is another, dissi-

pative mechanism that involves the polarization dependence of the nonlinear absorption. This mechanism can also occur in cubic crystals which lack birefringence. Nonlinear dissipative rotation of the polarization plane (referred to as NOA-2 for short) was first considered in Ref. 3.

Nonlinear optical activity is a very subtle but widespread phenomenon in nonlinear optics. Nonlinear optical activity due to various mechanisms is observable in crystals in 16 out of the 24 crystallographic classes possessing moderate or high degrees of symmetry; this suggests that the phenomenon should be useful in spectroscopy. The phenomenological and microscopic theories of NOA have been worked out fairly completely in Refs. 4–7; we are interested here in analyzing possible applications to spectroscopy.

Gallium arsenide is among the most interesting materials for analysis using nonlinear polarization spectroscopic techniques. The first experimental observations of NOA in GaAs at wavelength  $1.064\ \mu\text{m}$  were reported in Ref. 8. In our present work we used tunable picosecond light sources to analyze in detail the spectral dependence of the NOA and the nonlinear absorption in gallium arsenide near one- and two-photon resonances.

*Nonlocal nature of the nonlinear response in gallium arsenide.* We can treat the nonlocal nature of the of the nonlinear response in a crystal by adding terms involving spatial derivatives to the constitutive equation for the medium:

$$\begin{aligned} D_i = & \chi_{ij}^{(1)} E_j + \chi_{ijk}^{(2)} E_k E_j + \chi_{imkj}^{(3)} E_m E_n E_j \\ & + \dots + \gamma_{ijk}^{(1)} \nabla_k E_j + \gamma_{imjk}^{(2)} E_m \nabla_k E_j + \gamma_{imtjkh}^{(3)} E_m E_t \nabla_k E_j + \dots \end{aligned} \quad (2)$$

Here  $\mathbf{D}$  is the electric induction in the medium and  $\mathbf{E}$  is the field of the electromagnetic wave. The terms containing  $\hat{\chi}^{(3)}$  and  $\hat{\gamma}^{(3)}$  are cubic in the field and describe the self-action of the light (including the polarization self-action), i.e., processes that leave the frequency unchanged. There is no need to keep the terms involving the magnetic field of the light wave in this expansion—due to the coupling via the Maxwell

equations, the dependence on the magnetic induction can be regarded as a dependence on the spatial derivatives of the electric field.

Gallium arsenide belongs to the  $\bar{4}3m$  zincblende symmetry group, which has a plane of symmetry but no inversion center. Such crystals are isotropic:  $\chi_{ij}^{(1)} = \delta_{ij}\epsilon$ , and they have no gyrotropy:  $\gamma_{ijk}^{(1)} = 0$ . In weak light fields, the spatial dispersion shows up only in the second-order terms  $D_i \sim \eta_{ijkl}^{(1)} \nabla_k \nabla_l E_j$  and gives rise to a slight birefringence; however, for this birefringence the mirror axes of fourth-order symmetry coincide with the optic axes.<sup>9,10</sup>

To analyze the effects caused by the nonlocal nonlinear response in gallium arsenide, we begin by noting that in optically active crystals the rotation of the polarization plane depends on the  $\gamma_{123}^{(1)}$  tensor component,

$$\frac{d\varphi}{dz} = -\frac{\omega^2}{2c^2} \gamma_{123}^{(1)}. \quad (3)$$

In our case  $\gamma_{123}^{(1)} = 0$ , i.e., there is no gyrotropy in a weak light field, however, the contraction  $\gamma_{imijk}^{(3)} E_m E_l$  can be regarded (somewhat arbitrarily) as an "induced" tensor  $\tilde{\gamma}_{ijk}^{(1)}$ . For an intense light wave propagating in the  $\langle 001 \rangle$  direction and polarized along the  $\langle 100 \rangle$  axis, we have  $\tilde{\gamma}_{123}^{(1)} = 3\gamma_{11123}^{(3)} E_1 E_2^*$ ; however if the light is polarized along the  $\langle 010 \rangle$  axis, the sign of  $\tilde{\gamma}_{123}^{(1)}$  is different:  $\tilde{\gamma}_{123}^{(1)} = 3\gamma_{12223}^{(3)} E_2 E_1^* = -3\gamma_{11123}^{(3)} E_1 E_2^*$ , because for crystals in the  $\bar{4}3m$  class a tensor of rank 5 has only one nonzero independent component,<sup>11</sup> and  $\gamma_{11123}^{(3)} = -\gamma_{12223}^{(3)}$ . For different initial polarizations in gallium arsenide, the self-induced rotation due to the nonlocal nature of the nonlinear response may thus differ both in magnitude and in sign—the polarization vector rotates asymptotically either toward the bisector between the fourth-order symmetry axes of the crystal or toward the normal to this direction, depending on the sign of  $\gamma_{11123}^{(3)}$  (NOA-1):

$$\frac{d\varphi}{dz} = \frac{3\omega^2}{c^2} \gamma_{11123}^{(3)} |E|^2 \cos 2\Phi. \quad (4)$$

Here  $\Phi$  is the angle between the  $\langle 100 \rangle$  axis and the  $E$  vector of a wave of frequency  $\omega$  (Fig. 1). In the general case when the light travels along an arbitrary direction, the situation is more complicated; however, there is no rotation along the cubic third-order symmetry axes nor along the bisector between the fourth-order axes.

*Anisotropy of the cubic nonlinear susceptibility in gallium arsenide.* The third-order nonlinear susceptibility tensor in a cubic crystal is anisotropic—the nonlinear response depends on the polarization and direction of propagation of the light. The relation  $\chi_{1111}^{(3)} - \chi_{1212}^{(3)} - 2\chi_{1122}^{(3)} = 0$  characteristic of isotropic media does not hold for a cubic crystal. One of the consequences of the nonlinear anisotropy is that when light propagates along the  $\langle 001 \rangle$  axis, the two-photon absorption coefficient  $K_2$  is different for the polarizations  $E \parallel \langle 100 \rangle$  and  $E \parallel \langle 110 \rangle$ :

$$\begin{aligned} K_2(E \parallel \langle 100 \rangle) - K_2(E \parallel \langle 110 \rangle) &\propto \text{Im}\{\Delta\chi^{(3)}\} \\ &= \text{Im}\{\chi_{1111}^{(3)} - 2\chi_{1122}^{(3)} - \chi_{1212}^{(3)}\}. \end{aligned} \quad (5)$$

The polarization is preserved only for waves polarized along

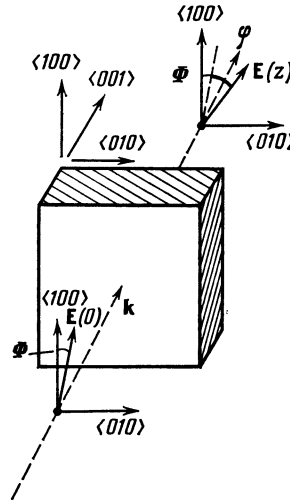


FIG. 1. Experimental configuration for recording the polarization self actions in a GaAs crystal.

the  $\langle 100 \rangle$ ,  $\langle 010 \rangle$ , or  $\langle 110 \rangle$  axes. In all other cases, the polarization vector rotates asymptotically toward the fourth-order axes or toward the bisectors between them, depending on the sign of the anisotropic component  $\Delta\chi^{(3)}$ ; this provides another mechanism for nonlinear gyrotropy (NOA-2) in gallium arsenide:

$$\frac{d\varphi}{dz} = \text{Im}\{\Delta\chi^{(3)}\} \frac{3\omega}{8nc} |E|^2 \sin 4\Phi. \quad (6)$$

A rigorous derivation of the formulas describing the dispersive and dissipative mechanisms of NOA can be found in Ref. 12. Here we note that natural optical activity shows up both as rotation of the plane of polarization  $\text{Re}\{\gamma^{(1)}\}$  and as circular dichroism  $\text{Im}\{\gamma^{(1)}\}$ . Similarly, NOA involves self-induced (intensity-dependent) rotation of the polarization plane accompanied by self-induced ellipticity. Expressions for the magnitude of the self-induced ellipticity can be derived from Eqs. (4) and (6) by interchanging the real and imaginary parts of the susceptibilities.

The phenomenon of self-rotation<sup>13</sup> of the polarization ellipse in nonlinear optics can occur in crystals of arbitrary symmetry, including ones with no nonlinear gyrotropy and no nonlinear anisotropy. This self-rotation is one of the manifestations of the high-frequency Kerr effect. This can be distinguished from NOA if we note that since no self-rotation of the polarization ellipse occurs for linearly polarized light, it can be neglected in experiments with linearly polarized light. In addition, the magnitude of the angle of the nonlinear rotation is independent of the initial orientation of the principal axes of the ellipse with respect to the crystallographic axes, and this fact is characteristic for the NOA mechanisms considered above and for crystals in the  $\bar{4}3m$  class.

The dissipative (NOA-2) and dispersive (NOA-1) mechanisms for nonlinear optical activity both occur concurrently and determine the contribution to the resultant nonlinear rotation angle and to the self-induced ellipticity. We can exploit the orientation dependence of the polarization self-rotation<sup>8</sup> (see Eqs. (4) and (6)) to distinguish

between effects due to nonlinear anisotropy and those due to the nonlocal character. We expect that the NOA-2 mechanism will dominate far from linear and nonlinear resonances in the absorption. An increase in the nonlinear rotation caused by the spatial dispersion of the nonlinearity may occur near exciton resonances. Indeed, we have

$$\frac{\varphi^{\text{NOA}-1}}{\varphi^{\text{NOA}-2}} \sim \frac{16\pi n \operatorname{Re}\{\gamma^{(3)}\}}{\lambda \operatorname{Im}\{\Delta\chi^{(3)}\}}, \quad (7)$$

while the order-of-magnitude estimate

$$\gamma^{(n)}/\chi^{(n)} \sim a \quad (8)$$

holds for the susceptibility, where  $a$  is a characteristic length in the crystal<sup>10</sup> (the lattice parameter in the nonresonant case, or the exciton radius  $a_{\text{exc}}$  for the case of resonance with an exciton transition). If we take  $\operatorname{Im} \Delta\chi^{(3)} \sim 0.5 \operatorname{Re} \chi^{(3)}$ ,  $a_{\text{exc}} \sim 1.5 \cdot 10^{-6}$  cm, and  $\lambda = 1.6 \mu\text{m}$  for purposes of estimate, we obtain

$$\varphi^{\text{NOA}-1} / \varphi^{\text{NOA}-2} \approx 1. \quad (9)$$

Near an exciton resonance in the absorption, NOA-1 and NOA-2 thus give comparable contributions and should therefore be readily distinguishable.

It should be borne in mind that in general, the nonlinear susceptibilities  $\chi^{(3)}$  measured in NOA spectroscopy are effective values, i.e., a sum of contributions from "direct" and "cascade" processes involving quadratic nonlinearities.<sup>1,2</sup> Cascade processes for  $\chi^{(3)}$  are forbidden for crystals belonging to the  $\bar{4}3m$  class.

## 2. PICOSECOND POLARIMETER-DENSITOMETER FOR NONLINEAR POLARIZATION SPECTROSCOPY OF CRYSTALS

The key device in NOA spectroscopy is the pulsed polarimeter, which is used to measure small ellipticities and rotations of the polarization plane. In most cases, the light remains almost linearly polarized after passing through the crystal. To identify nonlinear effects one must carry out measurements with different light intensities and crystal orientations in order to distinguish the contributions from the dissipative and dispersive NOA mechanisms. Concurrent measurements of the nonlinear absorption in crystals are also of interest. Pulsed lasers are needed to generate light

beams of high intensity, but they make it difficult to design tracking systems of the compensation type (the latter are well-suited for use with continuous light sources). These difficulties prompted us to develop a new method for carrying out pulsed polarization measurements which is suitable for highly precise measurements in nonlinear optics.

*Light source.* At present, parametric light generators are the only laser sources which combine adequate output power with tunability over the entire near-IR range, the region of greatest interest in experiments on the nonlinear optical properties of semiconductors. In our GaAs experiments we employed parametric light sources with LiNbO<sub>3</sub> and LiIO<sub>3</sub> crystals excited by pulses from a passively mode-locked YAG: Nd<sup>3+</sup> laser. The equipment included two amplifiers and a system for selecting a single laser pulse. The pulse length of the monitor laser was 35 ps. The laser operated stably over long periods, as required in spectroscopic studies—measurements of 100,000–150,000 pulses revealed that in 75% of the cases, the pulse energy deviated by less than 20% from the average pulse energy when the laser operated continuously at a frequency of 2.5 Hz. In the experiments in the 1.6–1.9  $\mu\text{m}$  region we used a two-stage superluminescence parametric light generator (PLG) with angular tuning and LiNbO<sub>3</sub> active crystals. The energy of the signal wave pulse from the PLG was  $\sim 100 \mu\text{J}$ , and the spectral width varied from 60  $\text{cm}^{-1}$  to 20  $\text{cm}^{-1}$  within the tuning range. The measurements at 0.8–0.9  $\mu\text{m}$  were made using a two-pass PLG with angular tuning; the generator used LiIO<sub>3</sub> crystals and was pumped by second-harmonic radiation from the YAG: Nd<sup>3+</sup> laser. The spectral width was 12  $\text{cm}^{-1}$ .

The light at the output of the PLG was spatially filtered to improve the accuracy of the spectroscopic data and make it easier to calculate the nonlinear optical susceptibilities. The spectral width and the wavelength were measured by a spectrometer.

*Optical system of the polarimeter-densitometer.* The polarimeter (Fig. 2) consisted of two calcite Glan prisms, which were mounted in a position corresponding to near-minimum transmission (the transmission when the polarimeter was "empty" was  $\sim 10^{-5}$  for all the wavelengths considered). The photoreceiver in channel C monitored the energy of the signal wave pulse from the PLG. The optical

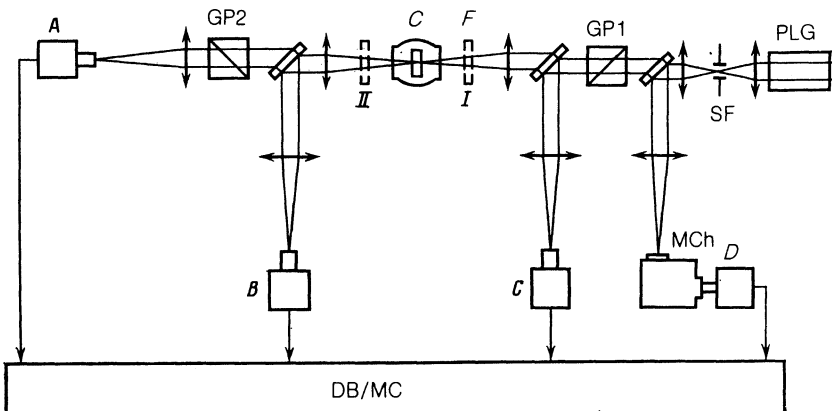


FIG. 2. Optical system of the polarimeter-densitometer. Photoreceivers A, B, C, and D are equipped with integrating illuminators; PLG is the light source (parametric light generator); SF, spatial filter; C, cryostat containing crystal; F, neutral optical filter; GP1 and GP2, polarizer and analyzer (Glan prisms); DB, data bus of microcomputer (MC); MCh monochromator.

density of the crystal was measured by analyzing the photoreceiver signals from channels *B* and *C*, while the photoreceivers in channels *B* and *A* were used in the polarization measurements. The energy of the laser pulses was recorded by infrared photoresistors or silicon photodiodes equipped with diffuse spherical illuminators. The latter effectively suppressed changes in the energy sensitivity of the photoreceiver channels when the transverse mode composition of the light changed or when the beam was slightly displaced during tuning of the PLG or realignment of the crystal. The crystal was immersed in a liquid nitrogen cryostat positioned in the focal plane of a telescope; the temperature in the cryostat was adjustable from 300 to 100 K.

The polarimeter-densitometer operated automatically under the control of a data acquisition system based on an "Elektronika D3-28" microcomputer. The system included strobed analog-to-digital transducers in the channels for measuring the energy of the laser pulses, servomechanisms with stepping motors and a monochromator, and controllers. This system enabled us to automatically align the crystal and set the wavelength of the light from the PLG.

**Measurement of the nonlinear absorption.** If the nonlinear absorption is measured using a single source, one must measure the optical density of the sample very accurately at several intensities and consider in detail the space-time profile of the beam and its transformation in the nonlinear crystal. In our experiments using integrating illuminators, the relative error in measuring the transmission coefficient of the crystal was less than 1%; it was determined not by the recording system but by fluctuations in the nonlinear absorption due to fluctuations in the length of the optical pulse. When a neutral glass light filter is moved from a position ahead of the crystal (I) to a position behind it (II) (Fig. 2), the radiation power density reaching the crystal increases, thereby changing the optical density of the crystal (due to nonlinear absorption) and thus altering the energy balance of the light pulses recorded in channels *B* and *C*. This change can be used to measure the nonlinear absorption.

**Polarimetry.** Moving the neutral filter from position I to position II changes the radiation power density at the crystal and thereby gives rise to an imbalance in the reference and signal arms of the polarimeter due to the induced nonlinear rotation  $\varphi$  and ellipticity *B*. If each measurement is carried out twice (once for each of two initial operating points symmetric about the minimum transmission point of the polarizer-analyzer-crystal system), one can obtain independent information on  $\varphi$  and  $|B|$  separately. Analysis shows that the sensitivity to the angle of nonlinear rotation is greatest if the tuning angle from the point of minimum brightness is equal to the square root of the residual transmission coefficient. Without optical compensators, this technique can be used only to find the ratio of the semiaxes of the polarization ellipse; the direction in which **E** moves along the ellipses (and hence the sign of *B*) cannot be determined.

One finds experimentally that the average nonlinear rotation angle is smaller than at the spatial and temporal center of the beam, and this fact must be borne in mind when analyzing the experimental data.

We define the specific self-induced ellipticity and rotation parameters  $D^{\text{NOA}}$  and  $C^{\text{NOA}}$  by

$$\begin{pmatrix} B \\ \varphi \end{pmatrix} = \begin{pmatrix} D^{\text{NOA}} \\ C^{\text{NOA}} \end{pmatrix} \int_0^l I(z, r, t) dz. \quad (10)$$

where *l* is the thickness of the crystal. In order to find the NOA constants (i.e., the function  $I(r, t, z)$ ), we calculated the spatial distribution of the light field in the crystal from measurements of the nonlinear absorption at the same light intensities recorded in the densitometric channel. To calculate the nonlinear absorption coefficient  $K_2$  and the specific nonlinear optical activity constants  $C^{\text{NOA}}$  and  $D^{\text{NOA}}$ , we used the following space-time model for the optical pulse:

$$I(0, r, t) = I_0 \exp(-r^2/r_0^2) \cos^2(t/\tau) \quad (11)$$

and neglected the self-focusing, which was justified for the crystal thicknesses used in the experiments. The procedure for calculating these parameters is extremely involved. It is described in detail in Ref. 14, which gives equations for  $K_2$  and formulas for calculating  $C^{\text{NOA}}$  and  $D^{\text{NOA}}$  from experimental data.

If the neutral filter is carefully selected (optical wedge, birefringence, nonuniformity of the optical density) our technique for measuring the nonlinear constants, in which the incident power density is changed by moving the filter from the forward to the backward positions relative to the crystal, effectively eliminates systematic errors in the optical and electrical portions of the measurement system, gives more accurate and reproducible results, and makes it possible to accurately record nonlinear rotation angles of the polarization plane as small as  $10^{-4}$  rad at all wavelengths of interest.

### 3. DISPERSION OF $\Delta\chi^{(3)}(\omega, \omega, -\omega, \omega)$ AND $\gamma^{(3)}(\omega, \omega, -\omega, \omega)$ NEAR ONE- AND TWO-PHOTON INTERBAND ABSORPTION RESONANCES

We studied the frequency dispersion of the nonlinear anisotropy and nonlinear gyrotropy in undoped GaAs single crystals near the two-photon ( $0.9E_g < 2\hbar\omega < 1.2E_g$ ,  $2\hbar\omega = 1.6E_g$ ) and one-photon ( $0.94E_g < \hbar\omega < E_g$ ) absorptions at 100 and 300 K ( $E_g$  is the width of the forbidden gap). The crystal thicknesses in the polarimetric and densitometric experiments ranged from 70  $\mu\text{m}$  to 3 mm, and the light propagated along the  $\langle 001 \rangle$  direction.

**Experiments at wavelength  $\lambda = 1.06 \mu\text{m}$   $T = 300$  K.** It is of interest to compare the orientation dependence for the angle of nonlinear rotation of the polarization plane and for the nonlinear absorption coefficients (Figs. 3 and 4, respectively). The amplitude spectrum of the "orientation harmonics" of these curves (the angles are defined as in Fig. 1) clearly demonstrates the advantages of polarimetry over densitometry in measurements of the nonlinear anisotropy—the signal/noise ratio in the polarimetric data is 20 times better than for the densitometric results, where information regarding the anisotropic component  $\hat{\chi}^{(3)}$  is obtained by directly measuring the polarization dependence of  $K_2$  (fourth harmonic, see Fig. 4)<sup>1)</sup> against an isotropic back-

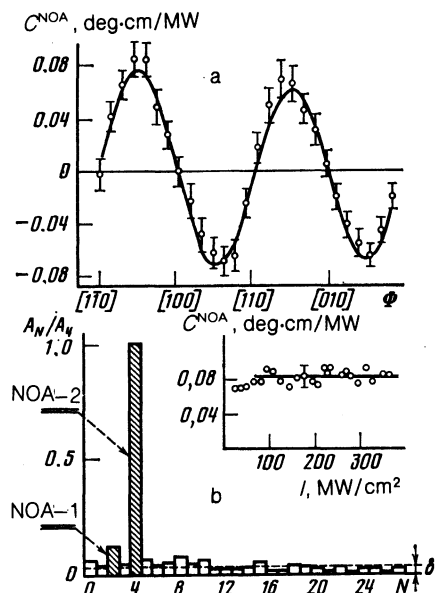


FIG. 3. a) Orientation dependence of the specific nonlinear rotation constant for NOA with  $k \parallel \langle 001 \rangle$ ;  $\varphi = \varphi(\Phi)$ , where  $\Phi$  is the angle between  $\mathbf{E}$  and the  $\langle 100 \rangle$  axis; b) Spectrum of the "orientation harmonics"  $\varphi(\Phi) = A_0/2 + \sum A_N \cos(N\Phi - \Psi_N)$ , where the  $A_N$  are the Fourier amplitudes for the orientation dependence in a). The contributions from NOA-2 ( $N = 4$ ) are distinctly visible, and there is a weaker contribution from NOA-1 ( $N = 2$ ).

ground component which corresponds to the zeroth harmonic in the spectra and is independent of orientation.

The nonlinear rotation angle saturates with intensity. At wavelength  $1.06 \mu\text{m}$  this occurs because two-photon absorption changes the effective nonlinear length of the crystal; this effect is included in the formulas for calculating the specific nonlinear optical activity  $C^{\text{NOA}}$ . For deep-band two-photon absorption at  $T = 300 \text{ K}$  we found that to within

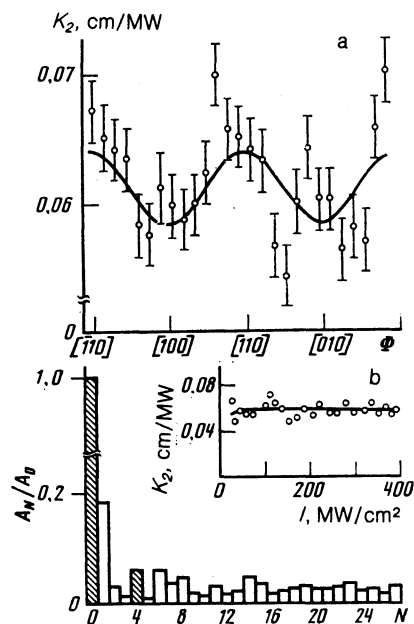


FIG. 4. a) Orientation dependence  $K_2 = K_2(\Phi)$  of the two-photon absorption coefficient for  $k \parallel \langle 001 \rangle$ . b) Fourier amplitudes for the orientation dependence in a); here the isotropic contribution ( $N = 0$ ) is dominant.

the experimental error, both  $C^{\text{NOA}}$  itself and the nonlinear absorption coefficient  $K_2$  (and thus the isotropic and anisotropic parts of the cubic nonlinear susceptibility) were independent of intensity in the range  $50\text{--}400 \text{ MW/cm}^2$  (Figs. 3, 4). Long term measurements in intense light at these wavelengths are not possible due to surface breakdown of the crystal.

#### Frequency dispersion of the nonlinear susceptibilities.

**Two-photon resonance.** The cubic nonlinear susceptibilities have a resonance peak when the frequency of the excitation light approaches the resonance frequencies for one- or two-photon absorption. Information on the real and imaginary parts of the susceptibilities, which describe the nonlinear gyrotropy and the anisotropy, can be obtained by measuring the nonlinear rotation of the polarization plane and the induced ellipticity for two different crystal orientations. The most convenient orientations are with the  $\langle 100 \rangle$  crystallographic axis making an angle  $\Phi = \pi/8$  or  $\Phi = -\pi/8$  with the polarization plane of the light, because in this case the NOA-1 and NOA-2 contributions add and subtract, respectively. Figure 5 plots  $\varphi$  and  $|B|$  near the two-photon absorption resonance at  $T = 100 \text{ K}$  for these two crystal orientations (here as everywhere in the experiments, the light traveled along the  $\langle 001 \rangle$  direction). Due to the absence of fundamental absorption in this frequency range, the nonlinear susceptibilities can be measured in a wide spectral interval.

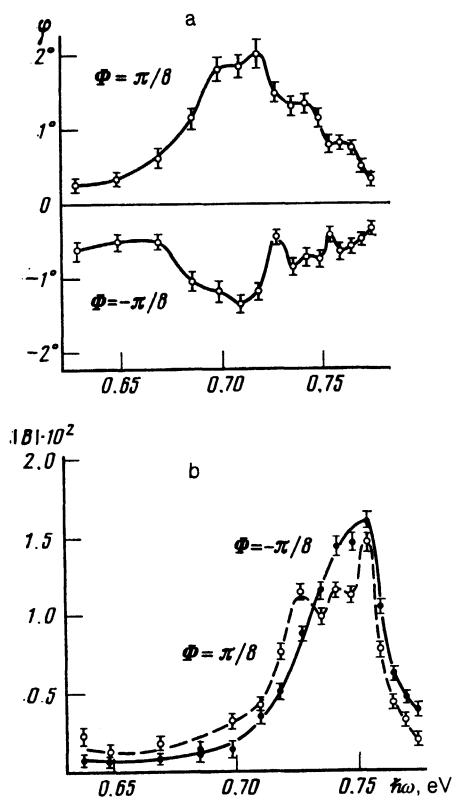


FIG. 5. Typical experimental curves for  $\varphi$  (a) and  $|B|$  (b) as functions of the photon energy  $\hbar\omega$  of the exciting light. In all cases  $T = 100 \text{ K}$ ,  $I = 200 \text{ MW/cm}^2$ .



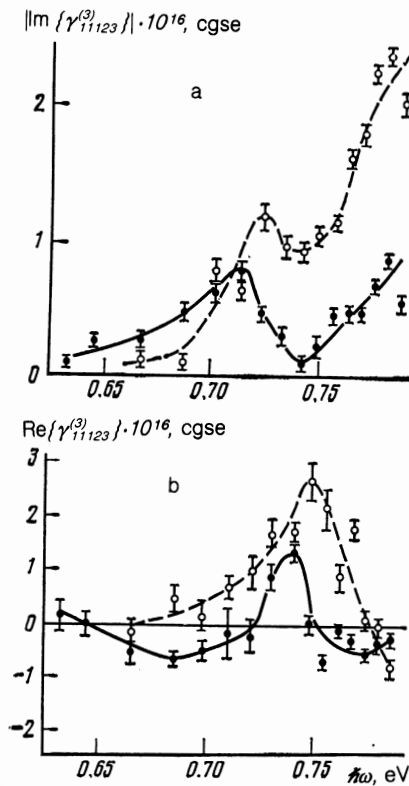


FIG. 7. Dispersion of the real part (a) and absolute value of the imaginary part (b) of the tensor  $\gamma^{(3)}$  near two-photon resonance in GaAs, measured at 300 K (●) and 100 K (○);  $I = 80 \text{ MW/cm}^2$  in all cases. The contribution from two-photon exciton resonance is evident.

100 K). Exciton lines were observed both in cold crystals ( $T = 100 \text{ K}$ ) and at room temperature  $T = 300 \text{ K}$  (Fig. 7). The resonance was shifted toward blue wavelengths and the exciton contribution increased when the crystal was cooled, because more time was required for the excitons to dissociate thermally in cold crystals. The width 0.02 eV of the observed exciton line was greater than the resolution of the equipment (determined by the width 0.007 eV of the parametric light generator) and was probably due to inhomogeneous broadening (and to collisional broadening at high free-exciton densities).

*Dispersion of the nonlinear rotation near the edge of the fundamental absorption band at  $T = 300 \text{ K}$ .* The specific nonlinear rotation of the polarization plane is found to be considerably greater near a one-photon interband resonance. The increase in the nonlinear rotation constant is probably due to the involvement of new transitions and to a change in the selection rules as compared with the case of two photon resonance. In addition, the close proximity of the one photon exciton resonance also plays a role. The orientation dependences of the nonlinear rotation angle and the self-induced ellipticity (Fig. 8), measured at  $\hbar\omega = 1.39 \text{ eV}$  in a crystal with  $l = 300 \mu\text{m}$ , indicate that the NOA-1 and NOA-2 mechanisms both contribute to the observed  $\varphi$ , and the relative contribution from NOA-1 is greater than for  $\hbar\omega = 1.16 \text{ eV}$ ,  $\lambda = 1.06 \mu\text{m}$  (cf. Fig. 3).

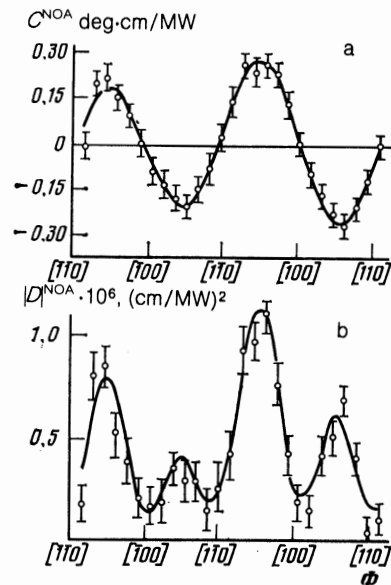


FIG. 8. Orientation dependence of the specific nonlinear rotation constant  $C^{\text{NOA}}$  for  $\mathbf{k} \parallel (001)$  (a) and the ellipticity  $D^{\text{NOA}}$  (b) near the absorption edge in GaAs ( $\hbar\omega = 1.39 \text{ eV}$ ,  $T = 300 \text{ K}$ ). Part b clearly shows the contribution from NOA-1 ( $N = 2$ ), cf. Figs. 3, 4.

#### 4. EFFECTS OF HIGHER NONLINEARITIES (SATURATION OF CUBIC NONLINEARITIES) IN POLARIZATION SPECTROSCOPY

The nonlinear rotations associated with one- and two-photon resonances can reach several degrees, and two-photon absorption at high excitation levels can dissipate much of the laser pulse energy. The question arises of the extent to which the cubic nonlinearities of spectroscopic interest can be measured accurately under these conditions. This problem was mentioned previously in Ref. 22, where nonadditive mixing of the contributions from the different NOA mechanisms was discussed, assuming strong nonlinear transformation of the polarization of the laser light. Numerical simulations show that nonadditive mixing can be neglected if the rotation angle is less than 1–2°. For semiconductors, the “turning on” of higher-order nonlinearities at high excitation levels is of greater practical importance. In particular, additional spectroscopic information should be obtainable from polarization measurements when higher-order nonlinearities are present.

We can use the experimental data to investigate this possibility. Figure 9 shows the frequency dispersions for the anisotropic part of the tensor  $\chi^{(3)}$  and the nonlinear absorption coefficient at two different intensities. Although the curves differ markedly, there share one feature in common—as the intensity increases, the susceptibilities saturate and the peak becomes much less pronounced. For example, a departure from the nonlinear absorption law:

$$dI/dz = -K_1 I - K_2 I^2 \quad (14)$$

was observed for a crystal excited near the edge of the two-photon absorption band.

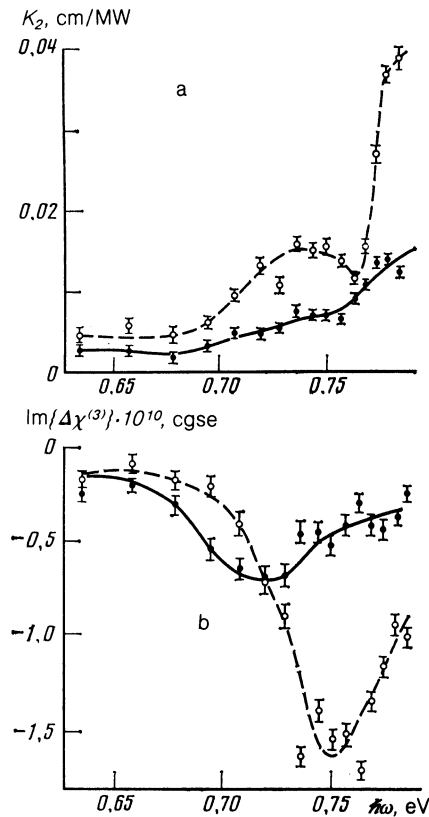


FIG. 9. Dispersion of the two-photon absorption coefficient  $K_2$  (a) and the anisotropic part of the imaginary part of the tensor  $\chi^{(3)}$  (b) measured at two intensities: 200 MW/cm<sup>2</sup> (O) and 600 MW/cm<sup>2</sup> (●). The saturation of the cubic nonlinearity at  $I = 600$  MW/cm<sup>2</sup> is evident (cf. Fig. 6).

#### Some mechanisms for higher nonlinearities: Estimates.

The saturation of the nonlinear susceptibilities (and in particular, the nonlinear absorption) cannot be attributed to higher-order nonlinear absorption processes involving three or more photons, because in this case the nonlinear absorption would increase, whereas our experimental results show that the susceptibilities saturate. Absorption due to free carriers becomes important when semiconductors are excited by laser pulses at optical wavelengths (particularly when the pulses are of nanosecond duration). The change in the light intensity  $I(z)$  during propagation in an undoped semiconductor caused by linear and nonlinear absorption, including absorption by free carriers, is described by the system of equations<sup>23</sup>

$$\frac{dI}{dz} = -K_1 I - K_2 I^2 - \Delta n \sigma I, \quad (15)$$

$$\frac{d\Delta n}{dt} = K_1 I / \hbar\omega + K_2 I^2 / 2\hbar\omega - \Delta n / \tau_R.$$

Here  $\sigma$  is the total absorption cross section for the free carriers, including absorption by free electrons and holes;  $K_1$  and  $K_2$  are the linear and nonlinear absorption coefficients, and  $\tau_R$  is the carrier recombination time. For a picosecond laser pulse in undoped GaAs the pulse is shorter than the interband relaxation time ( $\tau \ll \tau_R$ ), and to first order in the small parameter  $IK_2 z \ll 1$  system (15) simplifies to

$$\frac{dI}{dz} = -K_2 I^2 (1 + \sigma I \tau_R / 2\hbar\omega). \quad (16)$$

Here we have neglected the linear absorption  $K_1 z \ll 1$ , and the second term in parentheses on the right describes the relative contribution from absorption by free carriers to the dissipation of the laser pulse energy. Since  $\sigma \sim 5 \cdot 10^{-18}$  cm<sup>2</sup>,  $\hbar\omega \sim 1.4 \cdot 10^{-19}$  J, and  $\tau \sim 2 \cdot 10^{-11}$  s, we may neglect the absorption at excess light-induced carriers, at least up to 600 MW/cm<sup>2</sup>; indeed, (16) shows that this absorption should increase the observed value of  $K_2$  by  $\approx 20\%$ , whereas our experiments show that  $K_2$  decreased. Of course, excess carriers play an important role for longer optical pulses.

The above estimates ignore the change in the two-photon transition probability caused by the time-dependence of the population differences in the valence and conduction bands produced by the optical excitation. We can use the formula

$$\Delta n(t) = \frac{K_2}{2\hbar\omega} \int_{-\infty}^t I^2(t) dt \quad (17)$$

to estimate the number density of light-induced excess carriers generated by two-photon absorption. Here we can set  $K_2 \sim 0.04$  cm/MW,  $\hbar\omega \sim 1.4 \cdot 10^{-19}$  J, and  $\tau \sim 2 \cdot 10^{-11}$  s in our estimates. For excitation intensities  $I \sim 600$  MW/cm<sup>2</sup>,  $\Delta n$  exceeds  $10^{18}$  cm<sup>-3</sup>, which is high enough to make two-photon transitions much less probable. At these free carrier densities, a similar situation (referred to as band filling) occurs in many semiconductors (in particular, gallium arsenide) due to one-photon absorption<sup>24</sup>. Two-photon time-dependent changes in the population difference (two-photon band-filling) can be described using a direct-gap semiconductor model for which the excitation pulse length satisfies  $\tau_2 \ll \tau < \tau_R$ , where  $\tau_R$  and  $\tau_2$  are the interband recombination and dephasing times. If we solved the population rate equations simultaneously with Maxwell's equations, we find

$$\frac{dI}{dz} = -K_2 I^2 \exp\left(-\kappa K_2 \int_{-\infty}^t I^2(t) dt\right), \quad (18)$$

which differs from the "usual" relation for two-photon absorption.<sup>25</sup> If the intraband relaxation is rapid here:  $\tau \gg \tau_1$ , where  $\tau_1$  is the intraband energy relaxation time, then  $\kappa = (\hbar\omega \epsilon_0 g(\epsilon_0))^{-1}$ , where  $\epsilon_0 = (2\hbar\omega - E_g) / (1 + m_c / m_v)$ ; here  $m_c$  and  $m_v$  are the effective carrier masses in the valence and conduction bands, and  $g(\epsilon_0)$  is the number density of states at the energy  $\epsilon_0$ . We note that in a direct-gap semiconductor with a parabolic dispersion law, the saturation parameter  $\kappa K_2$  is insensitive to the excitation frequency (it decreases smoothly with increasing frequency). This behavior differs radically from the situation for one-photon resonance, for which saturation can occur only when  $\hbar\omega \approx E_g$ . Estimates using (18) reveal that the nonlinear absorption saturates significantly when the excitation intensity reaches  $I = 600$  MW/cm<sup>2</sup> ( $\tau = 20$  ps). This mechanism is quite general and should lead to saturation of the other cubic nonlinear susceptibilities associated with two-photon interband transitions. The saturation mechanism discussed above is apparently the dominant one for the crystals that we studied. In many cases it is important to investigate the saturation of the impurity levels that participate as intermediate resonances. The impurity levels are apparently responsible

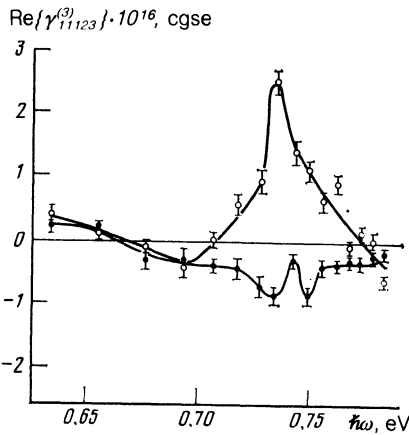


FIG. 10. Dispersion of  $\gamma^{(3)}$  in gallium arsenide measured at  $T = 100$  K for two intensities  $200 \text{ MW/cm}^2$  (O) and  $600 \text{ MW/cm}^2$  (●). The exciton resonance when  $I = 600 \text{ MW/cm}^2$  is almost completely suppressed (cf. Fig. 7).

for the nonmonotonic dependence of  $K_2$  on the wavelength at relatively low excitation intensities, and the filling of these levels at  $I = 600 \text{ MW/cm}^2$  "smooths out" this dependence (Fig. 9). It is helpful here to compare the anisotropic and isotropic parts of  $\chi^{(3)}$ . As was shown above, the impurity levels contribute little to the anisotropic component of the cubic nonlinear susceptibility. For this reason both  $\Delta\chi^{(3)}$  and  $K_2$  saturate in the same way; in both cases, the saturation occurs because the two-photon band filling makes two-photon transitions less likely. If transitions via impurity levels were important, the isotropic part of  $\chi^{(3)}$  would saturate more rapidly in a way that would depend on the wavelength.

The above results indicate that the "lattice-sensitive" interband transitions in gallium arsenide contribute decisively to the cubic nonlinearity for picosecond excitation

pulses of intensity up to  $600 \text{ MW/cm}^2$ , and the spectroscopic data adequately reflect the cubic nonlinearities of interest at excitation levels below a few hundred  $\text{MW/cm}^2$ , for which the free carriers and the saturation can be neglected.

**Screening of excitons.** The saturations of the discrete lines in the free exciton spectrum observed in polarization spectroscopy are of particular interest. Figure 10 shows the susceptibility  $\gamma^{(3)}$  near two-photon exciton resonance for several excitation levels at  $100 \text{ K}$  in a crystal of thickness  $2.5 \text{ mm}$ . Appreciable degradation of the exciton resonance sets in at intensities  $300\text{--}400 \text{ MW/cm}^2$ .

A "giant" polarization self-action is observed in the one-photon exciton resonance in thinner crystals ( $l = 70 \mu\text{m}$ ,  $T = 100 \text{ K}$ ).<sup>26</sup> The radiation leaving the nonlinear crystal is found to be strongly depolarized at  $\hbar\omega \approx 1.5 \text{ eV}$ .<sup>2)</sup> The depolarization is resonant in nature and increases up to an excitation level of  $10^{-4} \text{ J/cm}^2$ , at which the relative energy  $I_{\perp}/I_{\parallel}$  of the depolarized component reaches 10% (Fig. 11a). As the intensity of the excitation increases further, the excitation polarization becomes smaller and the line starts to disappear. As in the case of two-photon resonance, the estimated number density of free electrons at which appreciable degradation of the excitons lines sets in lies between  $10^{17}$  and  $5 \cdot 10^{17} \text{ cm}^{-3}$ . Comparing these results with data on the degradation of the exciton lines in the absorption spectra,<sup>29</sup> we conclude that the observed behavior can be attributed to dielectric screening of excitons.

We determined the nature of the observed depolarization by measuring the rotation of the polarization plane for the two crystal orientations  $\Phi = \pm \pi/8$ . The depolarized component was found to be associated primarily with a "pure" rotation of the polarization plane, and the NOA-1 and NOA-2 mechanisms both gave comparable contributions to the observed rotation. This permits us to estimate

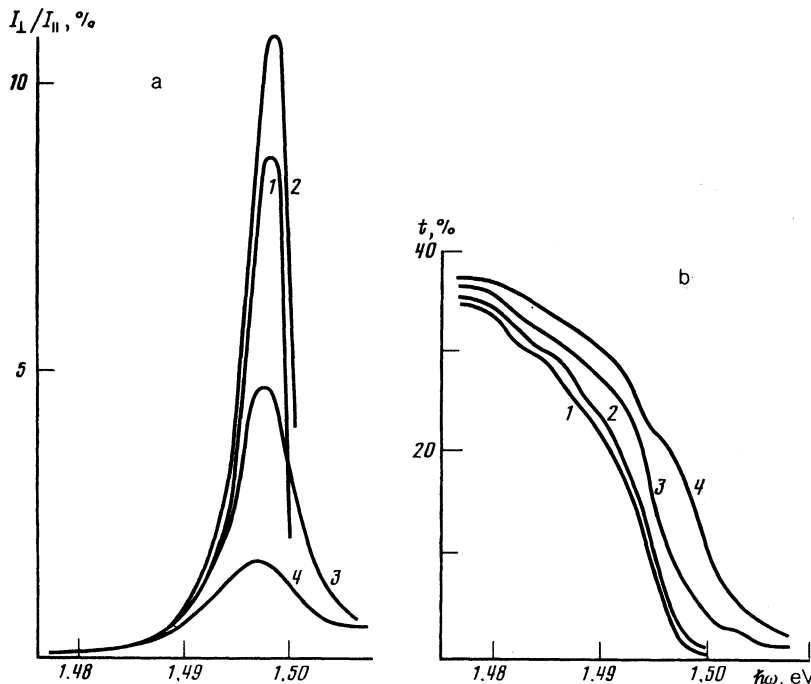


FIG. 11. a) Frequency dependence of the depolarized component of the light for four excitation levels near one-photon exciton resonance in GaAs. b) Transmission  $t$  of the crystal vs frequency at different excitation intensities. The nonlinear bleaching of the crystal with increasing excitation intensity is evident (cf. Ref. 24): 1)  $I = 4 \text{ MW/cm}^2$ ; 2)  $10 \text{ MW/cm}^2$ ; 3)  $32 \text{ MW/cm}^2$ ; 4)  $90 \text{ MW/cm}^2$ .

the corresponding nonlinear susceptibilities as follows:  $\text{Im}\{\Delta\chi^{(3)}\} \sim 10^{-7}$ ,  $\text{Re}\{\gamma^{(3)}\} \sim 10^{-13}$  (cgse units). These values are clearly somewhat low, since the depolarization was observed when the crystal was illuminated (Fig. 11b), while the exciton line remained well-defined up to excitation levels of  $1.5 \cdot 10^{-3}$  J/cm<sup>2</sup>. This polarization technique is thus uniquely suited for studying excitons and exciton screening.

## 5. CONCLUSIONS

The first experiments on nonlinear optical activity made it possible to identify the principal mechanisms for NOA. Since then, studies of polarization self-action have led to a new type of nonlinear spectroscopy for solids which yields unique information on the combined effects of spatial dispersion and nonlinearity and on the latent anisotropy in crystals. From the viewpoint of NOA spectroscopy, the most interesting materials are those with a pronounced spatial dispersion (such as copper chloride, with exciton and biexciton resonances, or highly nonlinear semiconductors with cubic symmetry, such as InSb and HgCdTe). For such crystals, polarization spectroscopy can yield better insight into the mechanisms responsible for the strong nonlinearity and enable one to ascertain the role of transitions involving free carriers. Crystals in the silver thiogallate family are especially well suited for studying the nonlinear gyrotropy—they have a large natural optical activity, the gyrotropy of the crystal depends on the electric field, and the NOA can be measured easily because there is no gyrotropy along the direction of the optic axis.<sup>30</sup> Frequency-nondegenerate NOA spectroscopy can also yield much new information; in this configuration, one linearly polarized ray at the “pump” frequency  $\omega_p$  alters the gyrotropy of the system, while a second weak ray at frequency  $\omega_{pr}$  serves as a probe. In this way one can analyze the complete spectra of the nonlinear susceptibilities  $\Delta\chi^{(3)}(\omega_{pr}, -\omega_p, \omega_p, \omega_{pr})$  and  $\gamma^{(3)}(\omega_{pr}, \omega_p, -\omega_p, \omega_{pr})$  and study how the resonant and nonresonant contributions interfere, just as in “active” Raman scattering spectroscopy. By choosing a configuration which is nondegenerate with respect to frequency or wave vector, one can use NOA spectroscopy to study the time-dependent nonlinear response and to directly record the relaxation times for the optically induced anisotropy and gyrotropy. Finally, reflection NOA spectroscopy can be employed in surface studies to analyze nontransparent as well as transparent crystals.

There is an acute need for a detailed quantum-mechanical theory of NOA, or more precisely, for a theory of nonlinear anisotropy and gyrotropy which is based on the actual band structure of crystals and treats the exciton and biexciton contributions. Studies of materials with a large NOA constant (and in particular gallium arsenide, which has a single-photon exciton resonance) will make it possible to develop a new class of devices in which one light beam is used to control another, and to create new logical and bistable optical devices for encoding data based on the polarization of light.

We express our sincere thanks to Z. M. Kostov for assisting us in this work and for a discussion of the results.

<sup>11</sup>We know of only one paper in which the polarization dependence of the nonlinear absorption was measured directly in a cubic crystal by using a single source.<sup>15</sup>

<sup>21</sup>A similar effect was observed previously at two-photon biexciton resonance in copper chloride.<sup>27,28</sup>

<sup>1</sup>S. A. Akhmanov and V. I. Zharikov, *Pis'ma Zh. Eksp. Teor. Fiz.* **6**, 644 (1967) [*JETP Lett.* **6**, 137 (1967)].

<sup>2</sup>P. W. Vol'kenshtein, *Molekulyarnaya Optika (Molecular Optics)*, Goskhozdat, Moscow (1961).

<sup>3</sup>M. I. Dykman and G. G. Tarasov, *Fiz. Tverd. Tela* **21**, 371 (1979) [*Sov. Phys. Solid State* **21**, 221 (1979)].

<sup>4</sup>P. W. Atkins and L. D. Barron, *Proc. Roy. Soc. A* **304**, 303 (1968).

<sup>5</sup>S. Kielich, *Opto-Electronics* **1**, 75 (1969).

<sup>6</sup>L. N. Avander and A. D. Petrenko, *Fiz. Tverd. Tela* **17**, 2263 (1975) [*Sov. Phys. Solid State* **17**, 1498 (1975)]; *Fiz. Tverd. Tela* **19**, 340 (1977) [*Sov. Phys. Solid State* **19**, 195 (1977)].

<sup>7</sup>S. A. Akhmanov, G. A. Lyakhov, V. A. Makarov, and V. I. Zharikov, *Opt. Acta* **29**, 1359 (1982).

<sup>8</sup>A. I. Kovrizhin, D. V. Yakovlev, B. V. Zhdanov, and N. I. Zheludev, *Opt. Comm.* **35**, 92 (1980).

<sup>9</sup>P. Y. Yu and M. Cordona, *Solid State Comm.* **9**, 1421 (1971).

<sup>10</sup>V. M. Agranovich and V. L. Ginzburg, *Kristallografika i Uchetom Prostranstvennoĭ Dispersii i Teorii Eksitonov (Crystal Optics with Spatial Dispersion and Theory of Excitons)*, Nauka, Moscow (1979).

<sup>11</sup>Yu. I. Sirotin and M. P. Shaskol'naya, *Osnovy Kristallografiki (Principles of the Physics of Crystals)*, Nauka, Moscow (1979), p. 286.

<sup>12</sup>N. I. Zheludev and A. D. Petrenko, *Kristallograf.* **29**, 1045 (1984) [*Sov. Phys. Crystallogr.* **29**, 613 (1984)]; *Opt. Acta* **31**, 1174 (1984).

<sup>13</sup>P. Maker, R. Terhune, and C. Savage, *Phys. Rev. Lett.* **12**, 507 (1964).

<sup>14</sup>R. S. Zadayan, *Nelineinaya Pikosekundnaya Poliarizatsionnaya Spektroskopiya Kristallov (Nonlinear Picosecond Polarization Spectroscopy of Crystals)*, Author's Abstract of Candidate's Dissertation, Moscow State University, Moscow (1985).

<sup>15</sup>S. J. Verko, *Phys. Rev.* **12B**, 669 (1975).

<sup>16</sup>S. A. Akhmanov, L. B. Meisner, S. T. Parinov, S. M. Saltiel, and V. G. Tunkin, *Zh. Eksp. Teor. Fiz.* **73**, 1711 (1977) [*Sov. Phys. JETP* **37**, 898 (1977)].

<sup>17</sup>L. B. Meysner, R. S. Zadayan, and N. I. Zheludev, *Solid State Comm.* **55**, 713 (1985).

<sup>18</sup>R. Baltramiunas, Yu. Vaĭtkus, and M. Pytrauskas, *Fiz. Tekh. Poluprovodn.* **16**, 1524 (1982).

<sup>19</sup>E. L. Ivchenko, S. A. Permogorov, and A. V. Sel'kin, *Solid State Comm.* **28**, 345 (1978).

<sup>20</sup>M. S. Brodin and Ya. O. Dovgikh, *Opt. Spektrosk.* **12**, 285 (1962).

<sup>21</sup>O. V. Gogolin, E. G. Tsitsishvili, Zh. L. Daĭs, K. Kliagskhiris, and V. E. Solomko, *Pis'ma Zh. Eksp. Teor. Fiz.* **34**, 328 (1980) [*JETP Lett.* **34**, 312 (1980)]; E. G. Tshitshishvili, O. V. Gogolin, J. L. Deiss, and V. N. Bagdavadze, *Solid State Comm.* **56**, 717 (1985).

<sup>22</sup>N. I. Zheludev, A. D. Petrenko, Yu. P. Svirko, and G. S. Filippova, *Izv. Akad. Nauk SSSR Ser. Fiz.* **48**, 601 (1984).

<sup>23</sup>C. R. Pidgeon, B. S. Wherret, A. M. Johnston, J. Dempsey, and A. Miller, *Phys. Rev. Lett.* **42**, 1785 (1979); **43**, 1843 (1980).

<sup>24</sup>J. L. Oudar, I. Abram, A. Migus, D. Hulin, and J. Etchepare, *J. Luminescence* **30**, 340 (1985).

<sup>25</sup>M. G. Dybenskaya, R. S. Zadayan, and N. I. Zheludev, *J. Opt. Soc. Am.* **2B**, 1174 (1985).

<sup>26</sup>N. I. Zheludev and Z. M. Kostrov, Preprint No. 34/1985, Phys. Dept., Moscow State Univ.

<sup>27</sup>T. Itoh and T. Kahotno, *J. Phys. Soc. Jpn.* **51**, 707 (1982); **54**, 2778 (1985).

<sup>28</sup>N. I. Zheludev, *J. Phys. Soc. Jpn.* **54**, 2777 (1985).

<sup>29</sup>G. W. Fehrenbach, W. Schäfer, and R. G. Ulbrich, *J. Luminescence* **30**, 154 (1985).

<sup>30</sup>S. A. Akhmanov and N. I. Zheludev, in: *Nonlinear Phenomena in Solids—Modern Topics*, World Science (1984), p. 233.

Translated by A. Mason